

# Single Frame Resection of Compact Digital Cameras for UAV Imagery

Martinus Edwin Tjahjadi

Department of Geodesy  
National Institute of Technology (ITN) Malang  
Malang, Indonesia  
edwin@lecturer.itn.ac.id

Fourry Handoko

Department of Industrial Engineering  
National Institute of Technology (ITN) Malang  
Malang, Indonesia

**Abstract**— Recently, UAVs (Unmanned Aerial Vehicles) gain a wider acceptance from many disciplines. One major application is for monitoring and mapping. Flying beyond eye sight autonomously and collecting data over large areas are their obvious advantages. To support a large scale urban city mapping, we have developed a UAV system which can carry a compact digital camera as well as a navigational grade of a Global Positioning System (GPS) board mounted on the vehicle. Unfortunately, such a navigational system fails to provide sufficient accuracy required to process images become a large scale map. Ubiquitous digital compact cameras, despite their low cost benefits, are widely known to suffer instabilities in their internal lenses and electronics imaging system. Hence these cameras are less suitable for mapping related purposes. However, this paper presents a photogrammetric technique to precisely determine intrinsic and extrinsic camera parameters of photographed images provided that sufficient numbers of surveyed control points are available. A rigorous Mathematical model is derived to compute each image position with respect to the imaging coordinate system as well as a location of the principal point of an image sensor and the focal length of the camera. An iterative Gaussian-Newton least squares adjustment method is utilized to compute those parameters. Finally, surveyed data are processed and elaborated to justify the mathematical models.

**Keywords**—interior orientation; UAV; collinearity; calibration; image processing

## I. INTRODUCTION

Recently, UAVs gain wider acceptance from many disciplines. One major application is for urban city mapping [1]. Flying beyond eye sight autonomously and collecting data over large areas are their obvious advantages. To support a large scale urban city mapping, we have developed an aerial mapping platform which is a remotely controlled fixed-wing plane that can carry a consumer grade camera as well as a navigational grade of a GPS board mounted on the aerial platform. Unfortunately, such a navigational system fails to provide sufficient accuracies required to process images become a large scale map [2]. Furthermore, Ubiquities digital compact cameras, despite their low cost benefits, have long been known to suffer unstable interior orientation (IO) elements [3-5]. For a nonmetric Sony Alpha 5100 camera used

in this research project, its IO parameters are not readily known with any precision. A position of the lens and its elements are located and aligned arbitrarily in a pre-defined location relative to the Charged Coupled Device (CCD) plane. In facts, deviations of the projected lens axis onto the CCD plane from the center of the sensor can be considerable amount of the extent of the sensor [6, 7]. This situation is unfavorable for a large scale mapping utilizing such cameras [8].

In photogrammetry and computer vision, the problem of spatial resection involves the determination of the spatial position and attitude of a camera or the image taken with that camera, with respect to the object space coordinate system [9]. It is solved with the aid of known coordinates of ground control points on the earth surface whose features appear on the image [10]. The orientation of the image is defined by the (IO) elements and the exterior orientation (EO) elements. The IO element comprises a focal length ( $c$ ) of the camera, and a principal point (PP) at  $H$  (Fig. 1). The focal length is defined as the perpendicular distance from the CCD sensor (i.e. image plane) to the focal node of the lens, while the location on the image where that perpendicular line intersects the image plane is termed as the PP of  $x_p$  and  $y_p$  [11], illustrated in Fig. 1.

In Figure 1, The EO elements of the camera are defined by six parameters, the three spatial coordinates of the camera (i.e.  $X_C, Y_C, Z_C$ ) with respect of a coordinate mapping system and three angular measurements which define the spatial orientation of the camera whilst taking a picture. The angular measurements are termed as  $\omega, \phi$ , and  $\kappa$  to indicate the rotations in a sequence order of the X, Y and Z axes respectively. These rotations are considered to be positive in a right handed sense relative to their respective axes. A coarse estimation of the EO parameters of each image is only available and can be computed using GPS telemetry navigational log data. The EO parameters for each overlapping images must be calculated in advance before commencing feature extraction process. Unfortunately, such a navigational system fails to provide sufficient accuracies required to process images become a large scale map.

Ministry of Research, Technology and Higher Education of the Republic Indonesia.

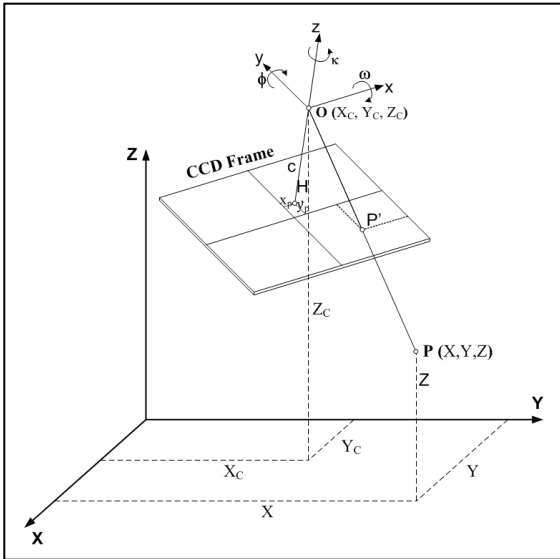


Fig. 1. A Collinearity Condition. (figure caption)

This paper discusses a development of a method of obtaining the PP, calibrated focal length of  $c$ , and EO parameters of the captured image with sufficient number of surveyed ground control points. Considering a collinearity condition as a functional model between the camera perspective center (O), portrayed control points on the image ( $P'$ ) and the respective ground control points (P), a recovery of the IO and EO parameter respectively can be achieved with sufficient accuracy for urban city mapping purposes.

A coarse estimation of the EO parameters of each captured image is only available and can be computed using GPS telemetry navigational log data. They must be calculated in advance before commencing feature extraction process. Accuracies of these data are not sufficient to further process images into a large scale map. Available geodetically observed GPS points that meet accuracy requirements are utilized to obtain the EO and IO parameters of UAV's images.

## II. RESEARCH METHOD

Assuming that a minimum number of five surveyed GPS control points are portrayed on the image, the EO and IO parameters can be computed by using a collinearity condition which stated that the perspective center (O), the image point ( $P'$ ), and the imaged object (P) all lie on a straight line [12]. This condition is used to develop the well-known collinearity equations which usually in the form of where the image coordinates of the imaged point are expressed as function of the IO and EO parameters:

$$\begin{aligned} x &= x_p - c \left[ \frac{r_{11}(X - X_C) + r_{12}(Y - Y_C) + r_{13}(Z - Z_C)}{r_{31}(X - X_C) + r_{32}(Y - Y_C) + r_{33}(Z - Z_C)} \right] \\ y &= y_p - c \left[ \frac{r_{21}(X - X_C) + r_{22}(Y - Y_C) + r_{23}(Z - Z_C)}{r_{31}(X - X_C) + r_{32}(Y - Y_C) + r_{33}(Z - Z_C)} \right] \end{aligned} \quad (1)$$

In order to evaluate the partial derivatives the expressions of the collinearity equation is rearranged as follows:

$$F = x = (x_p - c r/q); \quad G = y = (y_p - c p/q) \quad (2)$$

$$\begin{aligned} r &= r_{11}(X - X_C) + r_{12}(Y - Y_C) + r_{13}(Z - Z_C) \\ s &= r_{21}(X - X_C) + r_{22}(Y - Y_C) + r_{23}(Z - Z_C) \\ q &= r_{31}(X - X_C) + r_{32}(Y - Y_C) + r_{33}(Z - Z_C) \end{aligned} \quad (3)$$

In (1) and (2),  $x, y$  are the image coordinates of point  $P'$  on the image which relates the point P on the earth surface;  $X, Y, Z$  are the object space coordinate (i.e. WGS84 ECEF coordinate system) of point P.  $X_C, Y_C, Z_C$  are the object space coordinates of the camera position, whereas matrix elements of  $r_{11} \dots r_{33}$  are the coefficients of the orthogonal transformation between the image plane orientation and object space orientation. These elements constitute the exterior orientation parameter with rotation angles of  $\omega, \phi$ , and  $\kappa$  :

$$\mathbf{R} = \begin{bmatrix} r_{11} & r_{12} & r_{13} \\ r_{21} & r_{22} & r_{23} \\ r_{31} & r_{32} & r_{33} \end{bmatrix} \quad (4)$$

In which:

$$\begin{aligned} r_{11} &= \cos \phi \cos \kappa \\ r_{12} &= \sin \omega \sin \phi \cos \kappa + \cos \omega \sin \kappa \\ r_{13} &= -\cos \omega \sin \phi \cos \kappa + \sin \omega \sin \kappa \\ r_{21} &= -\cos \phi \sin \kappa \\ r_{22} &= -\sin \omega \sin \phi \sin \kappa + \cos \omega \cos \kappa \\ r_{23} &= \cos \omega \sin \phi \sin \kappa + \sin \omega \cos \kappa \\ r_{31} &= \sin \phi \\ r_{32} &= -\sin \omega \cos \phi \\ r_{33} &= \cos \omega \cos \phi \end{aligned} \quad (5)$$

When using a digital compact camera, the IO parameters are unstable between each exposure and it can be considered as unknowns. The collinearity equations are used to solve for the three unknown elements of the IO and the six unknown elements of the EO by developing a pair of equations for each of known ground control points. These equations are non-linear, for a solution of the non-linear equation using Newton's iterative method, almost invariably together with the method of least squares, one requires a linearization by the use of a Taylor series expansion of the function with respect to each of the unknown parameters. The result is a linear function, and (1) is linearized as follows[12]:

$$\begin{aligned}
 x - F_o &= (\partial F / \partial \omega)_o (\omega - \omega_o) + (\partial F / \partial \varphi)_o (\varphi - \varphi_o) \\
 &+ (\partial F / \partial \kappa)_o (\kappa - \kappa_o) + (\partial F / \partial X_C)_o (X - X_{C_o}) \\
 &+ (\partial F / \partial Y_C)_o (Y - Y_{C_o}) + (\partial F / \partial Z_C)_o (Z - Z_{C_o}) \\
 &+ (\partial F / \partial x_p)_o (x_p - x_{p_o}) + (\partial F / \partial y_p)_o (y_p - y_{p_o}) \\
 &+ (\partial F / \partial c)_o (c - c_o)
 \end{aligned} \quad (6)$$

$$\begin{aligned}
 x - G_o &= (\partial G / \partial \omega)_o (\omega - \omega_o) + (\partial G / \partial \varphi)_o (\varphi - \varphi_o) \\
 &+ (\partial G / \partial \kappa)_o (\kappa - \kappa_o) + (\partial G / \partial X_C)_o (X - X_{C_o}) \\
 &+ (\partial G / \partial Y_C)_o (Y - Y_{C_o}) + (\partial G / \partial Z_C)_o (Z - Z_{C_o}) \\
 &+ (\partial G / \partial x_p)_o (x_p - x_{p_o}) + (\partial G / \partial y_p)_o (y_p - y_{p_o}) \\
 &+ (\partial G / \partial c)_o (c - c_o)
 \end{aligned} \quad (7)$$

Equation (6) and (7) are a linearized form of (1) or (2) in terms of nine unknown parameters ( $\omega$ ,  $\varphi$ ,  $\kappa$ ,  $X_C$ ,  $Y_C$ ,  $Z_C$ ,  $x_p$ ,  $y_p$ , and  $c$ ).  $F$  and  $G$  denote the expression for  $x$  and  $y$ . Partial derivatives of  $F$  and  $G$  in the form of  $(\partial F / \partial a)_o$  and  $(\partial G / \partial a)_o$  are evaluated at each of the nine unknowns. Each of the partial derivatives “ $a$ ” is evaluated using the convergent or initial values of the variables and each of the terms, e.g.  $(\omega - \omega_o)$ . It can be considered as the corrections to be applied to the initial values, which are the unknown that are solved for. The  $F_o$  and  $G_o$  are the evaluation of the original function of  $F$  and  $G$  respectively with estimated values of the unknowns. Both represent the full respective function using all of the initial values in a linear function for a single point:

$$\begin{aligned}
 x - F_o + v_x &= b_{11}\Delta_\omega + b_{12}\Delta_\varphi + b_{13}\Delta_\kappa + b_{14}\Delta_{X_C} + b_{15}\Delta_{Y_C} \\
 &+ b_{16}\Delta_{Z_C} + b_{17}\Delta_{x_p} + b_{18}\Delta_{y_p} + b_{19}\Delta_c
 \end{aligned} \quad (8)$$

$$\begin{aligned}
 x - G_o + v_y &= b_{21}\Delta_\omega + b_{22}\Delta_\varphi + b_{23}\Delta_\kappa + b_{24}\Delta_{X_C} + b_{25}\Delta_{Y_C} \\
 &+ b_{26}\Delta_{Z_C} + b_{27}\Delta_{x_p} + b_{28}\Delta_{y_p} + b_{29}\Delta_c
 \end{aligned} \quad (9)$$

These equations use the shorthand notation of  $b_{ij}$  to indicate the partial derivatives of the original equations for the respective unknowns and use  $\Delta_{ij}$  to indicate the difference to be solved for. Variance terms  $v_x$  and  $v_y$  have been added when there are more equations than unknowns for allowing the least square solution.

System of linear equations (8) and (9) have nine unknowns based on  $n$  numbers of ground control points and it can be described as [12]:

$${}_{2n}\mathbf{L}_1 + {}_{2n}\mathbf{V}_1 = {}_{2n}\mathbf{A}_9 \quad {}_9\mathbf{X}_1 \quad (10)$$

where  $\mathbf{V}$  is the matrix of image observation residuals,  $\mathbf{L}$  is the matrix of the values of differences between calculated and

measured image coordinates, and  $\mathbf{X}$  is the correction matrix to the approximated unknown parameters. A linear least squares solution can be expressed as

$$\mathbf{X} = (\mathbf{A}^T \mathbf{P} \mathbf{A})^{-1} (\mathbf{A}^T \mathbf{P} \mathbf{L}) \quad (11)$$

where  $\mathbf{P}$  is the weighted matrix of the image measurements. The measurements are assumed uncorrelated between  $x$  and  $y$  coordinates, hence the weighted matrix for one point observation becomes:

$${}_2\mathbf{P}_2 = \begin{bmatrix} \sigma_x^2 & 0 \\ 0 & \sigma_y^2 \end{bmatrix} \quad (12)$$

The size of each matrix is determined by the number of ground control points available on the image. The matrix  $\mathbf{A}$ ,  $\mathbf{L}$ ,  $\mathbf{X}$  and  $\mathbf{V}$  respectively for  $n$  observed ground control points are illustrated as follows

$${}_{2n}\mathbf{A}_9 = \begin{bmatrix} {}_1b_{11} & {}_1b_{12} & \cdots & {}_1b_{17} & {}_1b_{18} & {}_1b_{19} \\ {}_1b_{21} & {}_1b_{22} & \cdots & {}_1b_{27} & {}_1b_{28} & {}_1b_{29} \\ {}_2b_{11} & {}_2b_{12} & \cdots & {}_2b_{17} & {}_2b_{18} & {}_2b_{19} \\ {}_2b_{21} & {}_2b_{22} & \cdots & {}_2b_{27} & {}_2b_{28} & {}_2b_{29} \\ \vdots & \vdots & \ddots & \vdots & \vdots & \vdots \\ {}_nb_{11} & {}_nb_{12} & \cdots & {}_nb_{17} & {}_nb_{18} & {}_nb_{19} \\ {}_nb_{21} & {}_nb_{22} & \cdots & {}_nb_{27} & {}_nb_{28} & {}_nb_{29} \end{bmatrix} \quad (13)$$

$${}_{2n}\mathbf{L}_1 = \begin{bmatrix} x_1 - x_p + c(r/q)_1 \\ y_1 - y_p + c(s/q)_1 \\ x_2 - x_p + c(r/q)_2 \\ y_2 - y_p + f(s/q)_2 \\ \vdots \\ x_n - x_p + f(r/q)_n \\ y_n - y_p + f(s/q)_n \end{bmatrix} \quad (14)$$

$${}_9\mathbf{X}_1 = [\partial\omega \quad \partial\varphi \quad \partial\kappa \quad \partial X_C \quad \partial Y_C \quad \partial Z_C \quad \partial x_p \quad \partial y_p \quad \partial c]^T \quad (15)$$

$${}_{2n}\mathbf{V}_1 = [v_{x_1} \quad v_{y_1} \quad v_{x_2} \quad v_{y_2} \quad \cdots \quad v_{x_n} \quad v_{y_n}]^T \quad (16)$$

The process of finding  $\mathbf{X}$  is iterative. The elements of matrices  $\mathbf{A}$  and  $\mathbf{L}$  are calculated according to initial estimates made of all nine unknowns. The corrected estimate values are applied to successive iteration until the corrections approach zero. This step is of paramount important since initial values differing too greatly from the actual ones could lead to a divergent solution. There are numerous methods are available

both in photogrammetric and computer vision communities respectively. The most comprehensive review of this method is outlined by [13], however reference [12-14] give a practical method for avoiding critical configuration of space resection. Nonetheless, computer vision literatures also contribute remarkable findings such as RANSAC [14], an Exact Solution [10, 15], a DLT like method [16, 17], a collinearity Constraint [18], and using a particular polynomial solver [19, 20].

### III. RESULT AND ANALYSIS

Two series of field observation was conducted in Malang city. First, establishment and measurement of 77 ground control points (GCPs) are conducted to provide reliable and precise control point coordinates. Each GCP are observed around 1 hour using geodetic type GPS instruments (Fig. 2). To give a possible highest accuracy of image coordinate measurements of control points on photographs, white concentric ring surrounded with dark background [21] is chosen and set up on the field (Fig. 3). In addition, aerial photography is conducted using three Sony Alpha 5100 cameras (Fig. 4) mounted on the fixed-wing UAV (Fig. 5).



Fig. 2. Base Stations of GPS observation



Fig. 3. Some of Ground control points on the field

The remotely controlled fixed-wing aero plane is utilized to capture around 160 images. Each ground control point on every image is identified, registered, and measured. This is to ensure that every identified ground control point on image must have its corresponding Earth Centered Earth Fixed (ECEF) coordinate of WGS84 datum on the ground (Fig. 6).



Fig. 4. Camera Sony Alpha 5100



Fig. 5. Aerial photography



Fig. 6. Some of Ground control points on the field appear on the captured image

Since the collinearity equation has 9 unknowns, only images which have a minimum 6 of control points are selected for computation only. This gives a minimum redundancy of a 3 degree of freedom. The averaged IO parameters are  $x_p = -0.420401\text{mm}$ ,  $y_p = -0.247472\text{mm}$ , and  $c = 15.488009\text{mm}$  respectively.

Table I shows some positional orientation parameter ( $X_C$ ,  $Y_C$ ,  $Z_C$ ) of images in terms of Cartesian WGS 84 reference frame. The standard deviation is in a range between 1mm to

5mm in all three directions of the axes. Meanwhile Table II presents some attitude parameters of the imaging camera while taking pictures. The standard deviation of the attitude is around 3 seconds.

TABLE I. TYPICAL VALUES OF CAMERA/PHOTO POSITION IN CARTESIAN COORDINATE SYSTEM

Image	Camera Position in WGS 84 Reference System		
	Xc (m)	Yc (m)	Zc(m)
1431	671634.024	9122876.340	812.7738
1439	671643.883	9122862.273	811.4944
1464	671631.378	9122875.622	813.9079
1590	671609.429	9122944.057	830.3971
1591	671610.774	9122955.242	827.7413
1592	671599.411	9122952.849	825.8397

TABLE II. TYPICAL VALUES OF CAMERA/PHOTO ATTITUDE

Image	Camera Attitude in Euler Rotation Angles		
	Omega - $\Omega$ (deg)	Phi - $\Phi$ (deg)	Kappa - $\kappa$ (deg)
1431	-1.9392	-10.2924	-12.5579
1439	6.5005	-2.7798	-69.9248
1464	-4.8714	3.0764	121.0954
1590	-2.9549	-1.5936	-3.6569
1591	-2.9689	-0.3637	-3.3654
1592	10.8635	-14.6889	-5.5099

#### IV. CONCLUSION

This paper has presented an optimization model for space resection using the collinearity condition that produce the interior and exterior orientation elements of each captured images of a digital compact camera which are computed simultaneously. It is clearly shows that all the orientation parameters of each image can be determined very accurately which meet mapping requirements related purposes. The algorithm is successfully implemented into C++ code, and it was tested and compare against proprietary photogrammetric software.

#### ACKNOWLEDGMENT

The author wishes to express his sincere thanks to Ministry of Research, Technology and Higher Education of the Republic of Indonesia for supporting a research grant “*Penelitian Terapan Unggulan Perguruan Tinggi (PTUPT)*”, with an announcement letter number 025/E3/2017 and a contract number 073/SP2H/K2/KM/2017.

#### REFERENCES

- [1] M. Saadatesherst, A. H. Hashempour, and M. Hasanlou, "UAV Photogrammetry: a Practical Solution for Challenging Mapping Projects," The International Archives of the Photogrammetry, Remote Sensing and Spatial Information Sciences, vol. XL(1/W5), pp. 619-623, 2015 2015.
- [2] J. Wang, M. Garratt, A. Lambert, J. J. Wang, S. Han, and D. Sinclair, "Integration of GPS/INS/vision sensors to navigate unmanned aerial vehicles," The International Archives of the Photogrammetry, Remote Sensing and Spatial Information Sciences, vol. XXXVII(B1), pp. 963-970, 2008.
- [3] D. C. Brown, "Close-Range Camera Calibration," Photogrammetric Engineering, vol. 37(8), pp. 855-866, 1971.
- [4] L. Ruizhi, Z. Hongran, L. Jian, and S. Yi, "Extrinsic parameters and focal length calibration using rotation-symmetric patterns," IET Image Processing, vol. 10(3), pp. 189-197, 2016.
- [5] Y. Zhang, L. Zhou, H. Liu, and Y. Shang, "A Flexible Online Camera Calibration Using Line Segments," Journal of Sensors, vol. 2016, pp. 1-16, 2016.
- [6] H. Hastedt and T. Luhmann, "Investigations on the quality of the interior orientation and its impact in object space for UAV photogrammetry," The International Archives of the Photogrammetry, Remote Sensing and Spatial Information Sciences, vol. XL(1/W4), pp. 321-328, 2015.
- [7] R. Wackrow, J. H. Chandler, and P. Bryan, "Geometric consistency and stability of consumer-grade digital cameras for accurate spatial measurement," Photogrammetric Record, vol. 22(118), pp. 121-134, 2007.
- [8] M. E. Tjahjadi, F. Handoko, and S. S. Sai, "Novel Image Mosaicking of UAV's Imagery Using Collinearity Condition," International Journal of Electrical and Computer Engineering (IJECE), vol. 7(3), pp. 1188-1196, June 2017.
- [9] M. Hamidi and F. Samadzadegan, "Precise 3D Geolocation of UAV Images using Georeferenced Data," The International Archives of the Photogrammetry, Remote Sensing and Spatial Information Sciences, vol. XL(1/W5), pp. 269-275, 2015.
- [10] M. E. Tjahjadi, "A Fast And Stable Orientation Solution of Three Cameras-Based UAV Imageries," ARPN Journal of Engineering and Applied Sciences, vol. 11(5), pp. 3449-3455, March 2016.
- [11] S. Konov and A. Gololobova, "Calibration of the Cameras of Photogrammetric Measurement Systems by Means of the Method of Least Squares," Measurement Techniques, vol. 57(6), pp. 639-642, 2014.
- [12] W. Förstner, B. Wrobel, F. Paderes, C. S. Fraser, J. Dolloff, E. M. Mikhail, and W. Rujikietgumjorn, "Analytical Photogrammetric Operations," in Manual of Photogrammetry: 6th Edition, J. C. McGlone, Ed. Bethesda, Maryland: American Society for Photogrammetry and Remote Sensing, 2013, pp. 785-955.
- [13] B. Haralick, C.-N. Lee, K. Ottenberg, and M. Nölle, "Review and analysis of solutions of the three point perspective pose estimation problem," International Journal of Computer Vision, vol. 13(3), pp. 331-356, December 1994.
- [14] M. A. Fischler, R. C. Bolles, and J. D. Foley, "Random Sample Consensus: A Paradigm for Model Fitting with Applications to Image Analysis and Automated Cartography," Communications of the ACM, vol. 24(6), pp. 381-395, 1981.
- [15] D. DeMenthon and L. S. Davis, "Exact and approximate solutions of the perspective-three-point problem," IEEE Transactions on Pattern Analysis & Machine Intelligence, vol. 14(11), pp. 1100-1105, 1992.
- [16] P. D. Fiore, "Efficient linear solution of exterior orientation," IEEE Transactions on Pattern Analysis & Machine Intelligence, vol. 23(2), pp. 140-148, 2001.
- [17] R. Samtaney, "A method to solve interior and exterior camera calibration parameters for image resection," Report No.NAS-99-003 NASA. Moffett Field, April 1999.
- [18] Y. Liu and H. Holstein, "Pseudo-linearizing collinearity constraint for accurate pose estimation from a single image," Pattern Recognition Letters, vol. 25(8), pp. 955-965, 2004.
- [19] H. Stewénius, D. Nistér, M. Oskarsson, and K. Åström, "Solutions to minimal generalized relative pose problems," in Workshop on omnidirectional vision, 2005, p. 6.
- [20] H. Zeng, "New Non-iterative Solution of the Perspective 3-Point Problem," Journal of Computational Information Systems, vol. 8(9), pp. 3747-3755, 2012.
- T. Clarke and X. Wang, "Extracting high-precision information from CCD images," in Proc. ImechE Conf., Optical methods and data processing for heat and fluid flow. City University, London, pp. 311-320, 1998.